ALMA Memo No. 500
Wind power spectrum near Chajnantor

Seiichi Sakamoto, Hideharu Ishizaki
National Astronomical Observatory of Japan
Mitaka, Tokyo 181-8588, Japan
and
Kotaro Kohno
Institute of Astronomy, University of Tokyo
Mitaka, Tokyo 181-0015, Japan

2004-05-31

Abstract

We present wind power spectral density up to ~ 1 Hz measured near Cerro Chajnantor. The power spectral density of variable component is represented by its value around 0.1 Hz. Median values of the wind power spectral density are smaller than those predicted by the Simiu model with a roughness length of 0.05 m in most cases. The 90-percentile values of the wind power spectral density are approximately three times larger than the corresponding median values. The wind power spectral density is not a simple function of mean wind velocity, and sometimes shows significant suppression after sunset. There exists no significant change of the wind power spectral density and roughness length that depend on the wind direction. Agreement of wind velocity measured at 8.0 m and 3.0 m above the surface within a few 10% difference supports small roughness length ($\ll 0.5$). The van der Hoven spectrum extracted from long-term weather station data implies that the weather system in this area is very stable and change of mean wind velocity (i.e., duration of gusty conditions) is dominated by the diurnal cycle.

1 Introduction

The ALMA antennas are exposed to wind loads, resulting in their deformation and pointing degradation. This effect can be significant for such large antennas operating at high frequencies, because they are subjected to larger loads due to their greater cross sections to the incident wind, and because they have greater risk of dynamic excitation due to their lower resonant frequencies[1], while they have smaller field of view requiring higher pointing accuracy.

The effects of wind on antennas are often calculated through finite element analysis using assumed static pressure distributions to predict deformation as functions of antenna elevation and wind incident angle. Prediction of pointing accuracy is more complicated task because it includes dynamic response of the structure and because our knowledge of the wind power spectrum is limited, and has so far been conducted based on simplified empirical spectra (e.g., Davenport 1962; Kaimal et al. 1972; Simiu & Scanlan 1978). However, in the early study by Holdaway et al. (1996), wind power spectral density at Llano de Chajnantor measured with a weather station was reported to have much flatter index of -1.04 in the spectral range from

[1]Given 12 m and 7 m as the diameters of the ALMA antennas, we expect their resonance frequencies to be 8 Hz and 14 Hz, respectively, from an empirical $(100\,\mathrm{m}/D)$ Hz scaling with the antenna diameter D (N. Ukita 2004, private communication).

0.01 to 0.1 Hz. We should thus check whether the wind contains significant energy out to antennas' structural resonant frequency (a few Hz) or not. Quantitative test of the Simiu spectrum assumed in the antennas' technical specification is of particular importance. Here we address these issues with a set of data measured near Cerro Chajnantor with better time response and longer period than the previous study by Holdaway et al. (1996) and provide information on the wind power spectral density additional to the very recent study by Beaupuits et al. (2004).

2 Instrumentation and Site

2.1 Higher Response Anemometer

We used a propeller-type anemometer with tail wind vane (Nippon Electric Instrument Inc. N-800S) installed atop an 8.0 m mast about 7 m to the south of the NAOJ site testing containers (Figure 1). This anemometer had a distance constant of 4 m (sea level value) and a 0.25 s sampling, both of which are better than those of the weather stations (5.2 m and 1200 s under regular operating mode) used to monitor the wind by Sakamoto et al. (2000). Although the adopted sampling rate of the weather station was determined by data storage limitation and thus, in principle, could be improved as high as 1/60 Hz, the rate is insufficient to deal with the 1 Hz component of wind power spectrum. Effects of natural vibration of the anemometer on gust power spectrum should be negligible in this study[2]. Measurable wind velocity range was 0.4–60 m s^{-1}. Specified accuracy was ± 0.5 m s^{-1} at ≤ 10 m s^{-1} and $\pm 5\%$ at ≥ 10 m s^{-1} in velocity, and $\pm 5^\circ$ in direction. The data sampled every 0.25 s were stored in a PC every second referring to the local civil time without summer time correction (UT $-$ 4h). The timing of the data acquisition referred to the internal clock of the PC, and there might be errors in timing up to several minutes. The anemometer has been operating at Pampa la Bola (4800 m above mean sea level) since 1999 March. The present analysis is based on the data taken during 1999 June 15 and 2000 February 12. Because of the power shortage, the data in the early morning are systematically missing, and there is no data taken between 6:00 and 9:00. The data set also contained noisy data particularly in winter afternoon, and we flagged out 1-hr periods with negative wind velocity from the analysis.

2.2 Weather Station

Independent wind data at the same site has been collected with a weather station placed at about 100 m to the northwest from the NAOJ site testing containers. The anemometer was Ogasawara Keiki WS-942 with a distance constant of 5.2 m (sea level value) set atop a 3.0 m mast. Measurable ranges were 2–60 m s^{-1} for wind velocity and 0–540° for wind direction. It records 1-min average wind velocity and instantaneous wind direction every 20 minutes referring to the local civil time without summer time correction (UT $-$ 4h). The accuracy of the wind velocity was specified to be ± 0.5 m s^{-1} at ≤ 10 m s^{-1} and $\pm 5\%$ at ≥ 10 m s^{-1}. The error of the repeatability of the wind direction measurement was specified to be $\pm 5^\circ$, though there might be systematic offsets up to 10° in the wind direction due to the uncertainty in setting the absolute position of the anemometer. Further technical details can be found in Sakamoto et al. (2000).

2.3 Site

Location of the instruments is shown in Figure 2 that illustrates local topography of the 19 $\times$ 18 km area including the Cerro Chascón science preserve. The most significant nearby obstacles

[2]Natural frequency of the first mode of vibration is estimated to be around 10 Hz for an 8.0 m steel (Young's modulus $\simeq 200 \times 10^9$ N m^{-2}) cantilever of a 0.08 m diameter with a 3 kg load at its free end.

for the N-800S anemometer are two 20 ft containers placed about 7 m to the north. Besides that, it is clear from this figure that the instruments are at downwind of the Cerro Chajnantor and Cerro Toco mountains but the upwind terrain is reasonably homogeneous and clear for about 3 km.

3 Results and Discussion

3.1 Wind Velocity and Direction

We summarize in Figure 3 combined plot of diurnal and seasonal variations of the 1-min average wind velocity measured with the weather station. The maximum 1-min average wind velocity recorded in 1999 with the weather station was $31.3\,\mathrm{m\,s^{-1}}$ on June 28 at 01:44. The year 1999 was ordinal in a sense that we confirmed the trend reported by Sakamoto et al. (2000) with the identical instrument. Namely, there are notable diurnal and seasonal variations in the wind velocity. The wind often starts blowing at around 9h in the morning and calms down at around 21h in the evening. The winter season (from May to November) is windier, with peak winds in June. The median wind velocity in 1999 was $6.5\,\mathrm{m\,s^{-1}}$, comparable to $7.0\,\mathrm{m\,s^{-1}}$ in 1997 (Sakamoto et al. 2000). The wind blows predominantly from the west, as shown in Figure 4. Occasionally, the wind blows from the east, but it is generally much weaker. Wind coming from either the north or the south is very rare.

The better response of the N-800S anemometer provides us better view of the wind characteristics at the site. Shown in Figure 5 are examples of the wind velocity and direction recorded on 1999 July 3, July 5, and August 7 with the N-800S anemometer and the weather station. These three days were selected because July 3 was one of the windiest days of the year, because July 5 showed sudden change of gustiness after sunset, and because August 7 showed change of wind direction. We confirmed both wind velocity and direction measured with the N-800S anemometer and the weather station reasonably agree, except that there is a systematic offset in the absolute values of the wind direction by about 10°.

3.2 Roughness Length

The lack of outstanding systematic difference of wind velocity measured at 3 m and 8 m is not an obvious result, and is useful to set an upper limit of the aerodynamic roughness length. Roughness length is the height above the ground surface at which the wind velocity is assumed to be zero when extrapolating the logarithmic wind velocity profile downward through the surface layer. Assuming the mixing is dominated by mechanical mixing due to shear forces, a relationship of mean wind velocity $\bar{v}$ with height z is derived as functions of the friction velocity v^*, the von Kármán constant k ($\simeq 0.4$), and the roughness length z_0 as $\bar{v} = (v^*/k)\ln[z/z_0]$ ("logarithmic profile"). The roughness length is a measure for the roughness of the terrain, and is ~ 0.0002 m for open sea, ~ 0.03 m for open country, and ≥ 2 m in centers of very large cities (Table 1), and the ratio of wind velocities at 8 m and 3 m is estimated to be 1.15 for $z_0 = 0.005$ m, 1.21 for $z_0 = 0.03$ m, and 1.55 for $z_0 = 0.5$ m. The observed small difference (less than a few times 10%) thus implies a small value ($\ll 0.5$ m) of the roughness length of logarithmic wind profile at the site. The data sets with more accurate relative calibration of wind velocity and synchronization, as well as larger height difference, are needed further determine the roughness length.

Table 1: Roughness lengths derived from the terrain classification of Davenport (Wieringa 1992)

Class	Surface	Landscape description	z_0 (m)
1	Sea	Open sea, fetch at least 5 km	0.0002
2	Smooth	Mud flats, snow; little vegetation, no obstacles	0.005
3	Open	Flat terrain; grass, few isolated obstacles	0.03
4	Roughly open	Low crops; occasional large obstacles	0.1
5	Rough	High crops; scattered obstacles	0.25
6	Very rough	Orchards, bushes; numerous obstacles	0.5
7	Closed	Regular large obstacle coverage (suburb, forest)	1.0
8	Chaotic	City center with high- and low rise buildings	>2

3.3 Wind Power Spectral Density

3.3.1 Models for Gust Spectrum

Wind power spectrum at frequencies above 0.01 Hz is often modeled by the empirical spectra such as those described in Davenport (1962) or in Kaimal et al. (1972) and Simiu & Scanlan (1978). In the Davenport model, the power spectral density is expressed as functions of the mean wind velocity $\bar{v}$ and the frequency f as,

$$S = \frac{4\kappa \bar{v}^2 x^2}{f(1+x^2)^{4/3}}, \tag{1}$$

where $x = (1200\,\mathrm{m})f/\bar{v}$, and κ is a dimensionless surface drag coefficient expressed as $[k/\ln(z/z_0)]^2$ with the von Kármán constant k ($\simeq 0.4$), the height z, and the roughness length z_0. An alternative is the Simiu model, for which the power spectral density is expressed as,

$$S = \frac{200\kappa z \bar{v}}{(1+50zf/\bar{v})^{5/3}}. \tag{2}$$

In the antennas' technical specification, the Simiu spectrum with the roughness length of 0.05 m has been assumed.

In Figure 6 we plotted curves of power spectral density in these models for different values of mean wind velocity and roughness length. In both models, the power spectral density at a given location is uniquely determined by mean wind velocity as long as the roughness length remains unchanged. The power index at higher frequency range gradually approaches to the Kolmogorov's $-5/3$ exponent ($\propto f^{-5/3}\ \bar{v}^{8/3}$), which is characteristic to three-dimensional isotropic turbulence in the inertial subrange. The most significant difference is the existence of a turnover of the power spectral density at around 0.01 Hz in the Davenport model.

3.3.2 Effects of Distance Constant of Anemometer

Wind velocity is observed through the filter of the anemometer response. Because propeller-type anemometers are first-order lag systems with non-zero distance constants — the length of fluid flow past the sensor required to cause it to respond to $1 - 1/e$ (63.2%) of the increasing step-function change in velocity — there should be systematic underestimation of wind power at lower wind velocity and higher frequency ranges as well as phase delay. The specified distance constant of the N-800S anemometer was 4 m at sea level, and is expected to be 7.3 m at 4800 m due to the reduced air density, though the actual value might be better. The frequency response

function is expressed as $[1 + (2\pi f l_0/\bar{v})^2]^{-1/2}$ with the distance constant at the site l_0, mean wind velocity $\bar{v}$, and the frequency f (Kristensen & Hansen 2002). At higher frequency range, the response factor varies as $\propto (f/\bar{v})^{-1}$, and thus the observed power spectral density at higher frequency may vary as $\propto f^{-8/3}\ \bar{v}^{11/3}$. Estimated power spectral density suppression due to this effect is overlaid in Figure 6. At velocities larger than $8\,\mathrm{m\,s^{-1}}$, the effects of distance constant is smaller than a factor of a few in frequency range smaller than 0.1 Hz.

3.3.3 Power Spectral Density of Variable Component

Power spectral density of variable component was extracted from the N-800S anemometer data. We conducted an FFT analysis and obtained the square of the amplitude A^2, as a function of the frequency f every 1.14 hr (4096 s). The power spectral density S is then calculated as $A^2/\Delta f$, where Δf is the sampling frequency multiplied by the number of data points used in the FFT.

The power spectral density, which is represented by the samples shown in Figures 7–9, was smaller than those predicted by the Davenport and Simiu models in most cases. Flattening of the power spectral density at lower frequencies occurs at around 0.005 Hz or lower and the flattening point roughly scales with the mean wind velocity. At around 0.2 Hz or higher, the power index becomes steeper ($\simeq -8/3$), with the drop-off frequency roughly scaling with the mean wind velocity. This drop-off may be artifact due to the non-zero distance constant of the N-800S anemometer described in the previous subsection though the drop-off frequency appears significantly higher than the prediction probably because of the better response of the anemometer than the specifications. Flattening of the power spectral density at the high frequency end primarily observed under low wind conditions is attributed to the $1/f$ white noise. No hint of effects of natural vibration of the anemometer was observed in the spectra.

The wind power spectral density significantly scatters, and for some fraction of time, the power becomes considerably higher than the median values. This is demonstrated in Figure 10 by plots of cumulative fraction of wind power spectral density computed from 128 data points around 0.1, 0.2, 0.5 and 1 Hz taken during a 9.1-hr period starting from 10:00 of 1999 July 3. The 90-percentile value at a certain frequency is typically a factor $\simeq 3$ larger than the corresponding median value. Namely, if we adopt a power spectral density 4 times larger than the median value obtained by this study, the wind power is smaller than the adopted value for more than 90% of time.

To summarize, the power spectral density of variable component can be represented by the median power spectral density of the frequency component well above the flattening point, and under the restrictions of the anemometers' frequency response, we conclude that the representing frequency is around 0.1 Hz.

3.3.4 Diurnal and Seasonal Distribution of Gusty Conditions

Provided that the power spectral density of variable component is represented by the value at 0.1 Hz, we can track time distribution of gusty conditions. Shown in Figure 11 is a combined plot of diurnal and seasonal variations of the 1.14-hr median wind power spectral density at 0.1 Hz measured with the N-800S anemometer. This plot mimics that of the mean wind velocity shown in Figure 3. Namely, the power spectral density of variable component is traced by mean wind velocity as a first order approximation, supporting the assumption of both of the models in section 3.3.1 that the wind power spectral density is a unique function of mean wind velocity as long as the height and the roughness length are unchanged. Quantitative comparison of the data with the model prediction demonstrates that the models with a roughness length of 0.05 m reproduce the $\bar{v}^{8/3}$ dependence of the power spectral density at higher frequency except for a factor ~ 5 difference in absolute values (Figure 12).

A closer comparison of the data with the models demonstrate, however, the existence of sudden suppression of wind power spectral density after sunset by a factor > 10 without significant change of mean wind velocity and direction (Figure 8). The median wind power density at 0.1 Hz is not a simple function of mean wind velocity but sometimes reduces suddenly after sunset (Figures 5, 8, 12). The difference between the first and second half-night is not significant in this context. We additionally note that the wind is more turbulent than the model prediction in the morning when the wind is calm ($< 5\,\mathrm{m\,s^{-1}}$). The latter phenomenon may be attributed to contribution of thermally induced turbulence trapped below the surface inversion layer.

As for the topographic effects, no significant difference of power spectral density depending on wind direction was observed (Figure 9).

3.3.5 Longer Term Variability

The time series of wind fluctuations measured with the weather station can also be transformed into a power spectrum for evaluation of longer-term variability of wind velocity in a manner described by van der Hoven (1957).

In the combined non-normalized wind spectrum measured with the weather station during a period from 1998 November 1 to 2000 February 1 and those taken with the N-800S anemometer (Figure 13), several distinct energy peaks and gaps are apparent. The first peak is at 1.16×10^{-5} Hz, which corresponds to the diurnal cycle. Although we expected a major peak lower than this, which corresponds to the transit period of fully developed weather systems such as depressions and is usually called the macro-meteorological peak, we found it is very weak if any. Lack of a significant macro-meteorological peak suggests that the weather system in this area is very stable and change of mean wind velocity is dominated by the diurnal cycle. At higher frequency, there exists a broad peak at around 0.01 Hz, which is associated with the turbulence of the boundary layer, and is termed the micrometeorological peak. The well-defined gap between these two peaks is called the spectral gap in which there is little fluctuation over a range of frequency of about one order of magnitude. The spectral gap is an important feature since it conveniently separates atmospheric motion into two distinct categories, i.e., turbulence with locally stationary statistical properties and quasi-steady mean velocities associated with slowly varying synoptic or climatological timescales.

4 Summary and Future Work

We monitored wind velocity and direction near Cerro Chajnantor and deduced wind power spectral density up to ~ 1 Hz. The power spectral density of variable component was found to be represented by its frequency component around 0.1 Hz. Median values of the wind power spectral density after correction for the anemometer response were smaller than those predicted by the Simiu model with a roughness length of 0.05 m in most cases. The 90-percentile values of the wind power spectral density were approximately three times larger than the corresponding median values. The wind power spectral density is not a simple function of mean wind velocity but sometimes shows significant suppression after sunset. There exists no significant change of the wind power spectral density and roughness length that depend on the wind direction. Agreement of wind velocity measured at 8.0 m and 3.0 m above the surface within a few 10% difference supports small roughness length ($\ll 0.5$). The data sets with more accurate relative calibration of wind velocity and synchronization, as well as larger height difference, are needed further determine the roughness length. The van der Hoven spectrum extracted from long-term wind data taken with the weather station implies that the weather system in this area is very stable and change of mean wind velocity (i.e., duration of gusty conditions) is dominated by the diurnal cycle.

Obviously, measurements at the Chajnantor site with an ultrasonic anemometer of higher response installed atop a rigid-enough mast are meaningful. Quantitative evaluation of the increase of roughness length due to adjacent antennas will be important for evaluating pointing degradation of the ALMA antennas in their most compact configuration. We foresee these analysis with an ultrasonic anemometer next to the ASTE telescope at Pampa La Bola. The latter study may also be possible with an existing anemometer placed adjacent to the prototype antennas at the ALMA Test Facility.

We thank ALMA-J site testing team who jointly established and maintained the anemometer and collected the data in Chile with us. We also thank Ichiro Tamagawa of Gifu University and Nobuharu Ukita for advices.

References

[1] Beaupuits, J. P. P., Otárola, A., Rantakyrö, F. T., Rivera, R. C., Radford, S. J. E., & Nyman, L.-Å. 2004, "Analysis of wind data gathered at Chajnantor", ALMA Memo 497

[2] Davenport, A. G. 1961, "The spectrum and horizontal gustiness near the ground in high winds", Quart. J. Royal Meteorol. Soc., 87, 194

[3] Holdaway, M. A., Foster, S. M., Emerson, D., Cheng, J., & Schwab, F. 1996, "Wind velocities at the Chajnantor and Mauna Kea sites and the effect on MMA pointing", ALMA Memo 159

[4] Kaimal, J. C., Wyngaard, J. C., Izumi, Y., & Coté, O. R. 1972, "Spectral characteristics of surface layer turbulence", Quart. J. Royal Meteorol. Soc., 98, 563

[5] Kristensen, L., & Hansen, O. F. 2002, "Distance constant of the Risø cup anemometer", Risø-R-1320(EN) (Roskilde: Risø National Laboratory)

[6] NRAO 1999, "Topographical map of CONICYT science preserve"

[7] Sakamoto, S., Handa, K., Kohno, K., Nakai, N., Otárola, A., Radford, S. J. E., Butler, B., & Bronfman, L. 2000, "Comparison of meteorological data at the Pampa La Bola and Llano de Chajnantor sites", ALMA Memo 322

[8] Simiu, E., & Scanlan, R. H. 1978, "Wind effects on structures", (New York: John Wiley and Sons)

[9] van der Hoven, I. 1957, "Power spectrum of horizontal wind speed in the frequency range from 0.007 to 900 cycles per hour", J. Meteorol., 14, 160

[10] Wieringa. J. 1992, "Updating the Davenport roughness classification", J. Wind Eng. Aerod., 41, 357

Figure 1: The N-800S anemometer installed atop an 8.0 m mast at Pampa La Bola as seen from southwest (photo as of 2000 February 6). The most significant nearby obstacles are two 20 ft containers ($6.06 \times 2.49 \times 2.50$ m) placed about 7 m to the north.

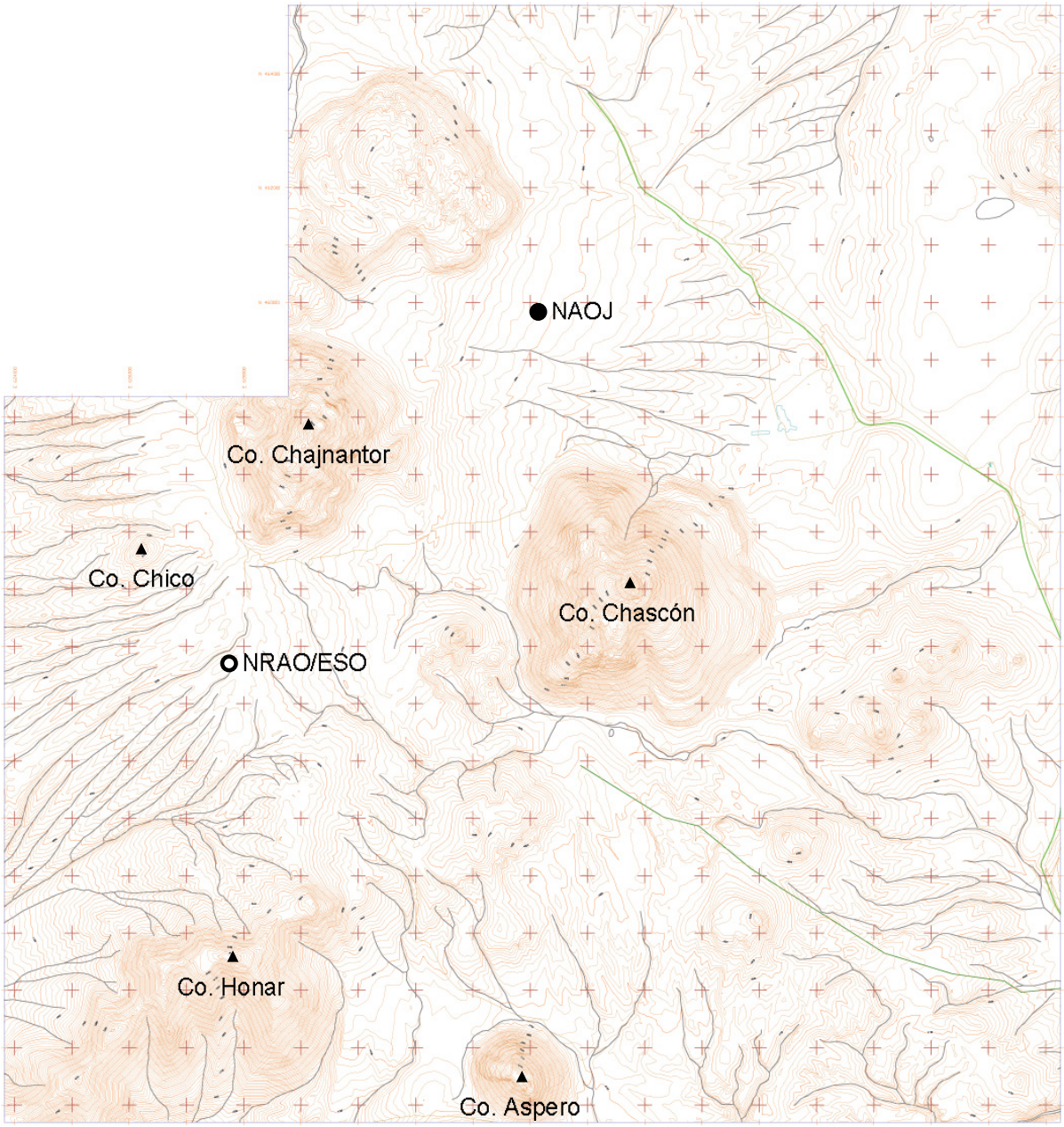

Figure 2: Location of the NAOJ instruments at Pampa La Bola (alt.$\simeq$ 4800 m; *filled circle*) used in this work as well as that of the NRAO/ESO instruments at Llano de Chajnantor (alt.$\simeq$ 5050 m; *open circle*), overlaid on the map of the 19×18 km area including the Cerro Chascón science preserve, produced from aerial photographs by McLain Aerial, Tucson, for NRAO, NRO, and ESO. North is to the top and east is to the left. Ticks are spaced every 1 km. Contour spacing is 10 m with thick contours every 50 m. The nearby peaks including Cerro Chascón and Cerro Chajnantor are indicated with filled triangles. Cerro Toco is to the northeast of Cerro Chajnantor, midst the top left corner area where the map is missing. Note that the predominant wind blows from west, and the upwind terrain of the NAOJ instruments is reasonably homogeneous for about 3 km.

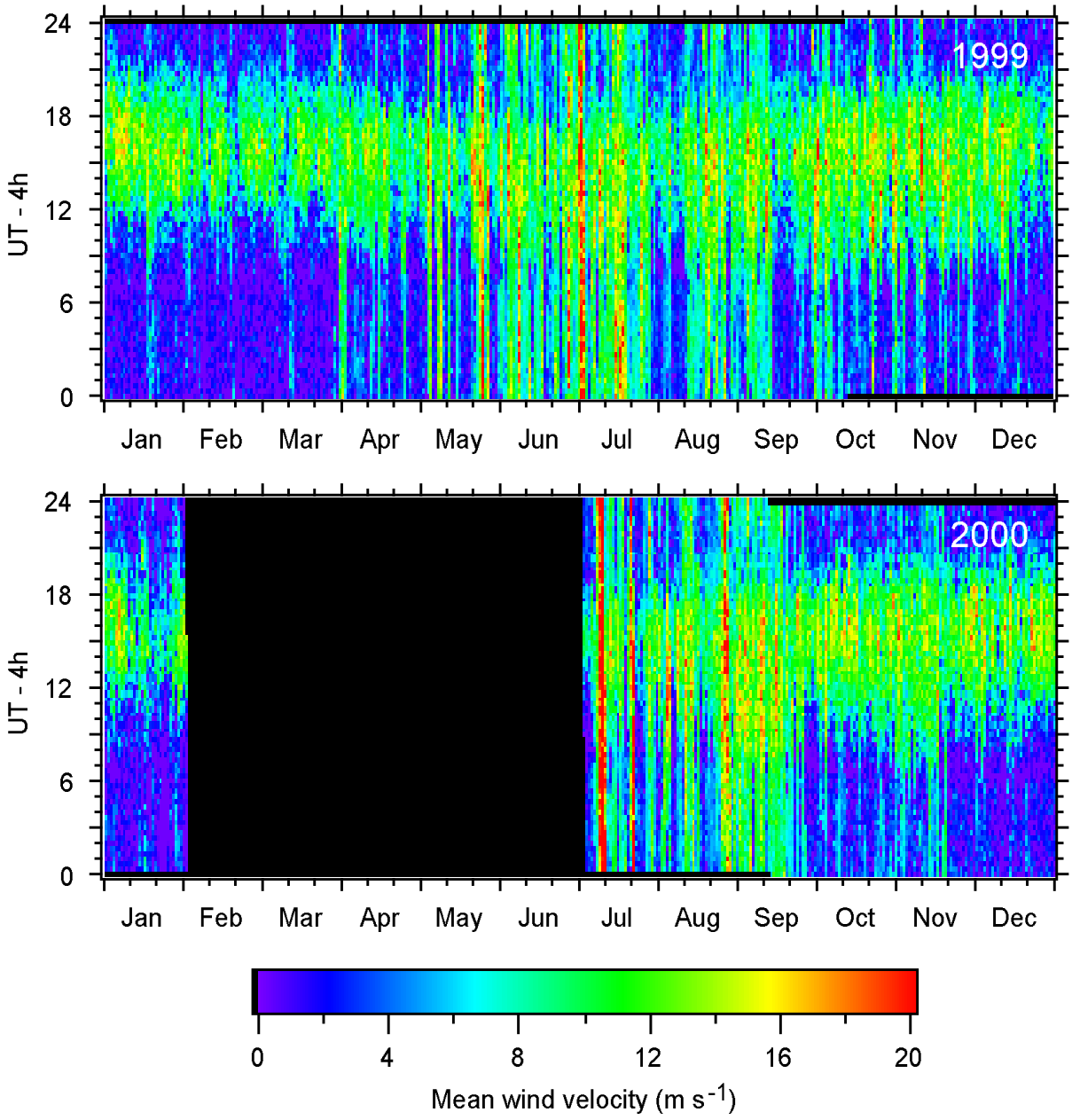

Figure 3: Combined diurnal and seasonal variation plot of 1-min average wind velocity sampled every 20 min taken with the weather station used by Sakamoto et al. (2000). The instrument was not operating during the period coded in black. The plot is for the years 1999 and 2000 while the entire data set covers longer period.

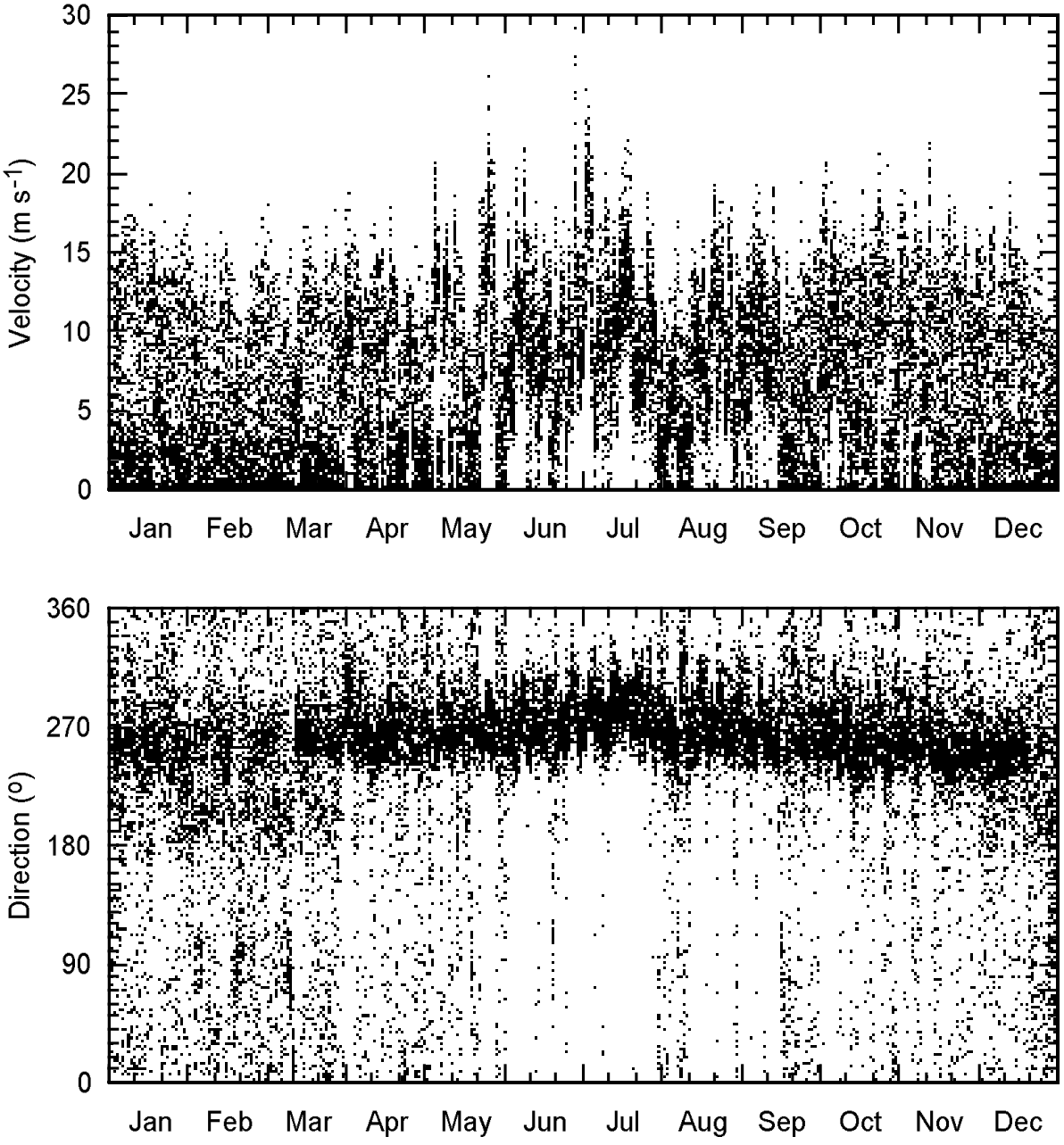

Figure 4: Wind velocity and direction in 1999 monitored with the weather station. North is 0° and east is 90°. Note that the absolute values of the wind direction may include systematic offsets of up to 10° due to an uncertainty in the absolute direction setting.

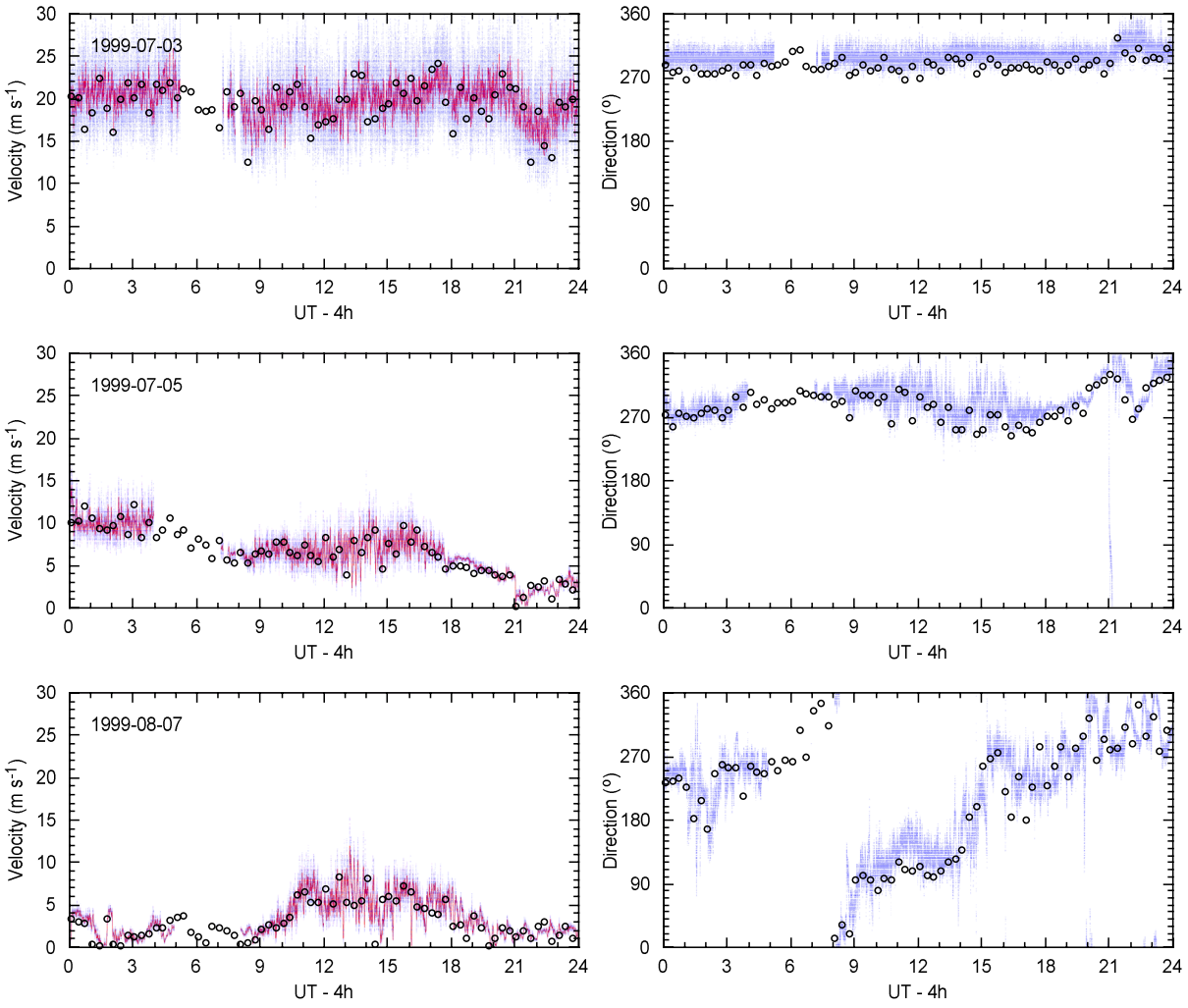

Figure 5: Example of the wind velocity and direction on 1999 July 3, July 5, and August 7 taken with the N-800S anemometer atop an 8 m mast and the weather station atop a 3 m mast. North is 0° and east is 90°. Open circles denotes weather station data. Blue lines are for the N-800S anemometer instantaneous data, with their 1-min running mean shown in red lines.

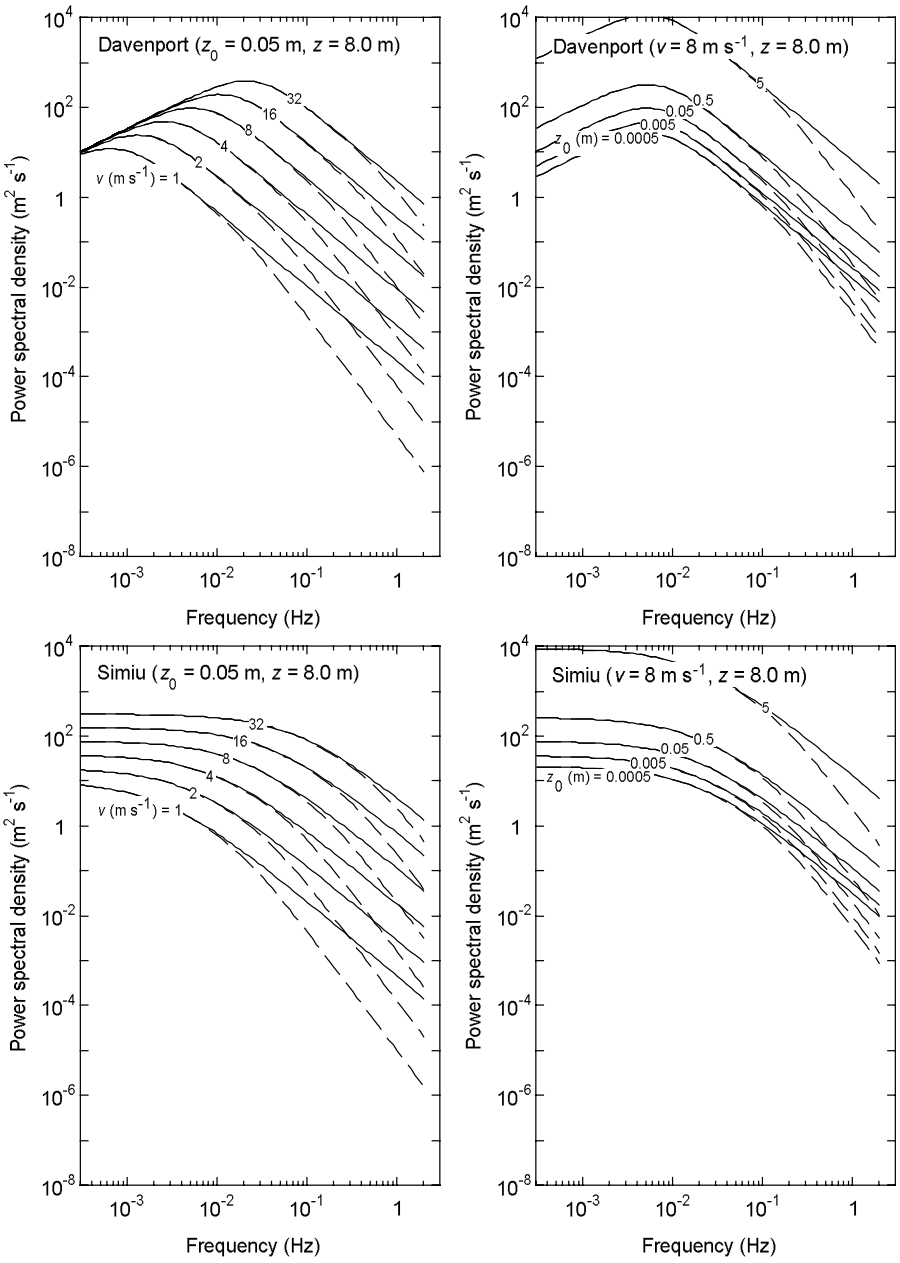

Figure 6: The wind power spectral density for different values of mean wind velocity and roughness length expected from the empirical Davenport model (*top*: Davenport 1961) and the Simiu model (*bottom*: Kaimal et al. 1972; Simiu & Scanlan 1978). Dashed lines are corresponding simulated spectra measured with an anemometer with a distance constant of 7.3 m.

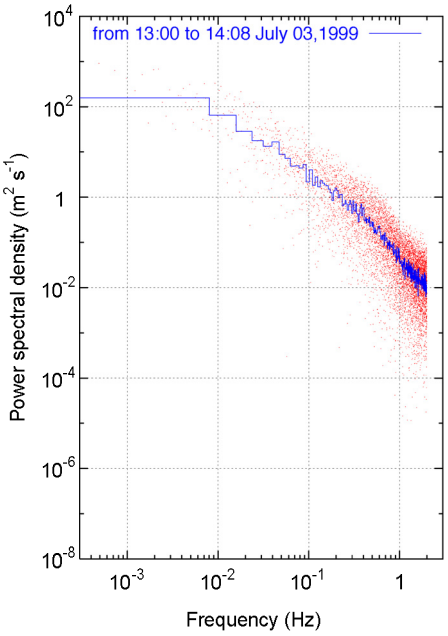

Figure 7: Wind power spectral density extracted from the N-800S anemometer data taken during a 1.14-hr period starting at 13:00 on 1999 July 3 (UT − 4h), one of the windiest periods of the year. Mean wind velocity was 19.9 m s^{-1}. Red dots indicate power spectral density, and the blue line indicate the median values calculated every 32 samples.

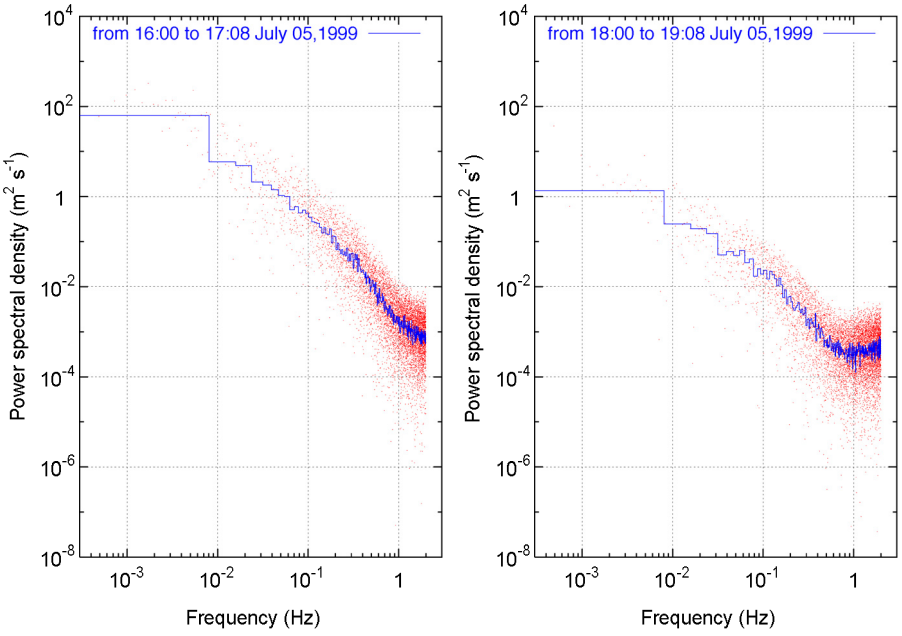

Figure 8: Same as Figure 7 but for 1.14-hr periods starting at 16:00 and 18:00 on 1999 July 5. Mean wind velocity during these periods were 7.32 and 5.78 m s^{-1}, respectively.

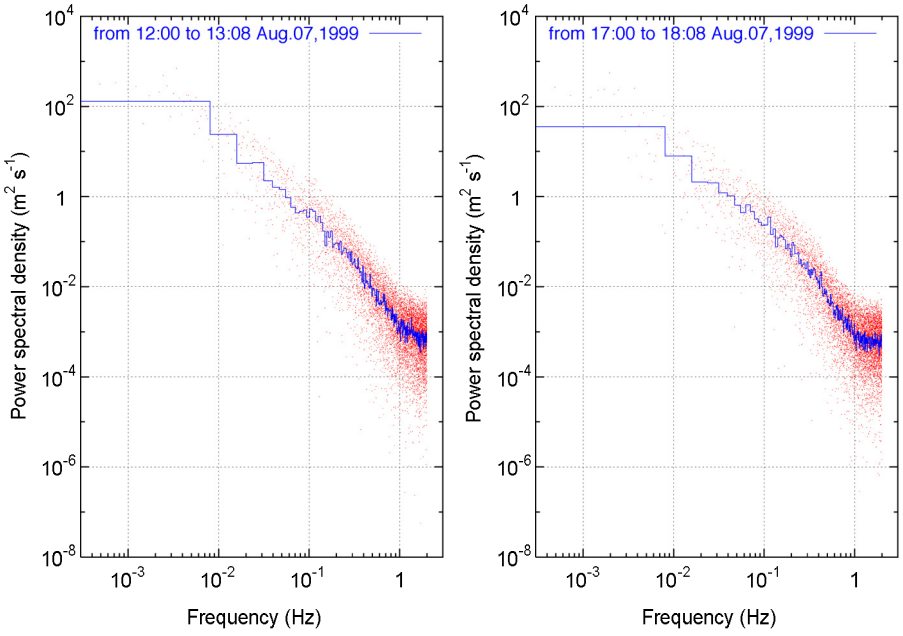

Figure 9: Same as Figure 7 but for 1.14-hr period starting at 12:00 on 1999 August 7, when the east wind was dominant, and that starting at 17:00 of the same day, when the west wind was dominant. Mean wind velocity during these periods were 5.45 and 5.42 m s^{-1}, respectively.

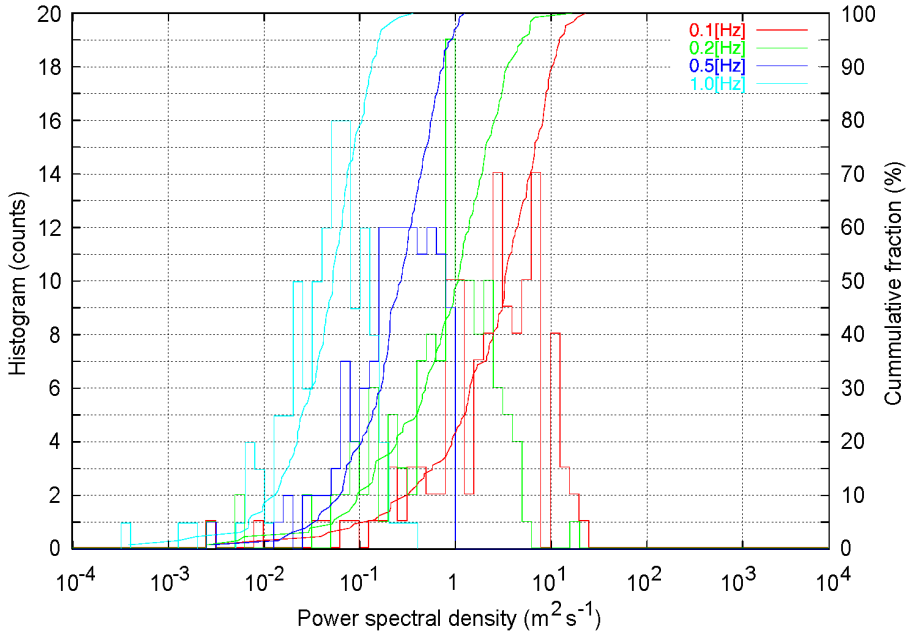

Figure 10: Histogram and cumulative fraction of wind power spectral density computed from 128 data points around 0.1, 0.2, 0.5 and 1 Hz taken during a 9.1-hr period starting from 10:00 of 1999 July 3. The 90-percentile value at a certain frequency is typically a factor $\simeq 3$ larger than the corresponding median value.

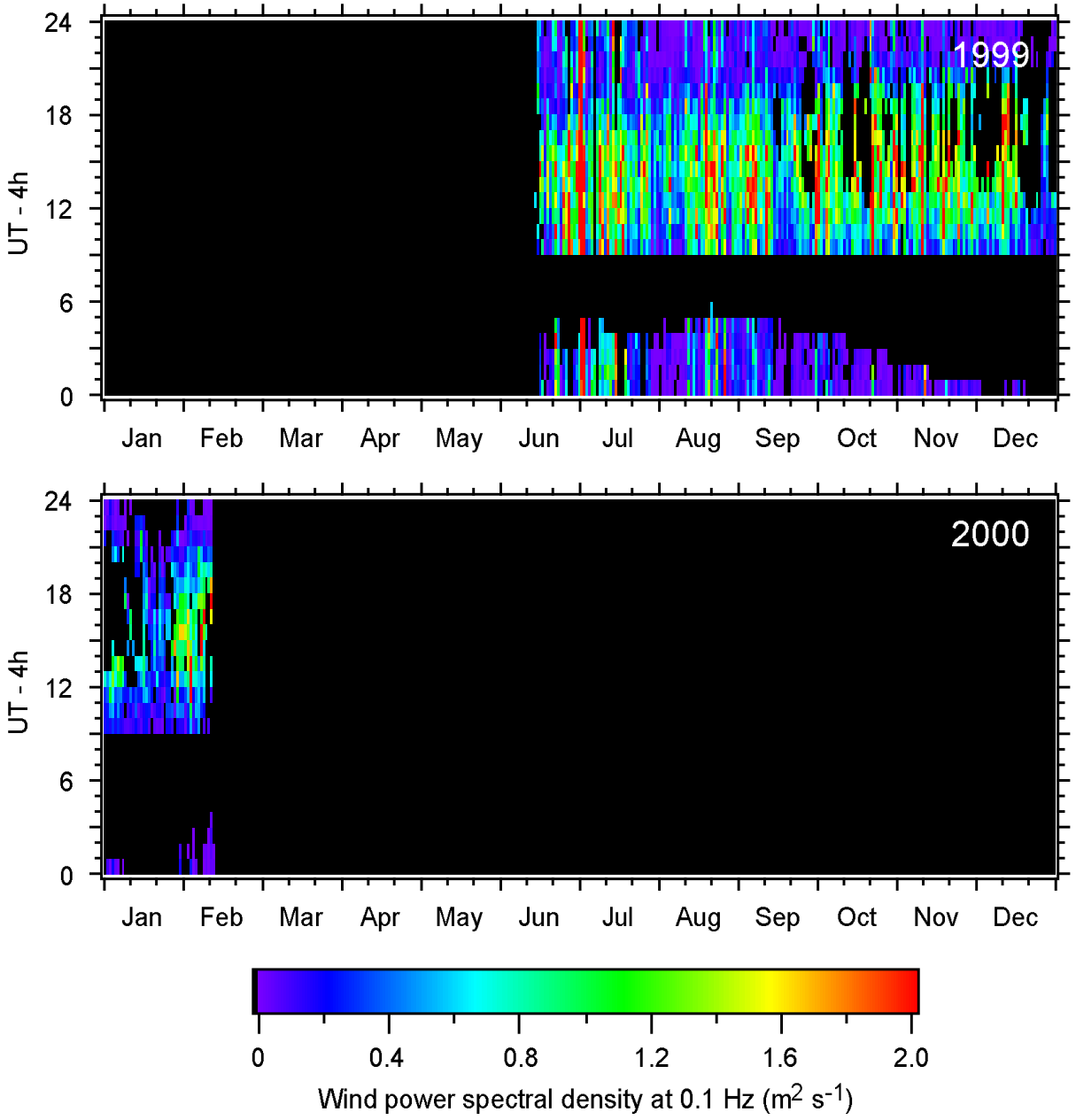

Figure 11: Combined diurnal and seasonal variation plot of wind power spectral density at 0.1 Hz. The instrument was not fully operating during the periods coded in black.

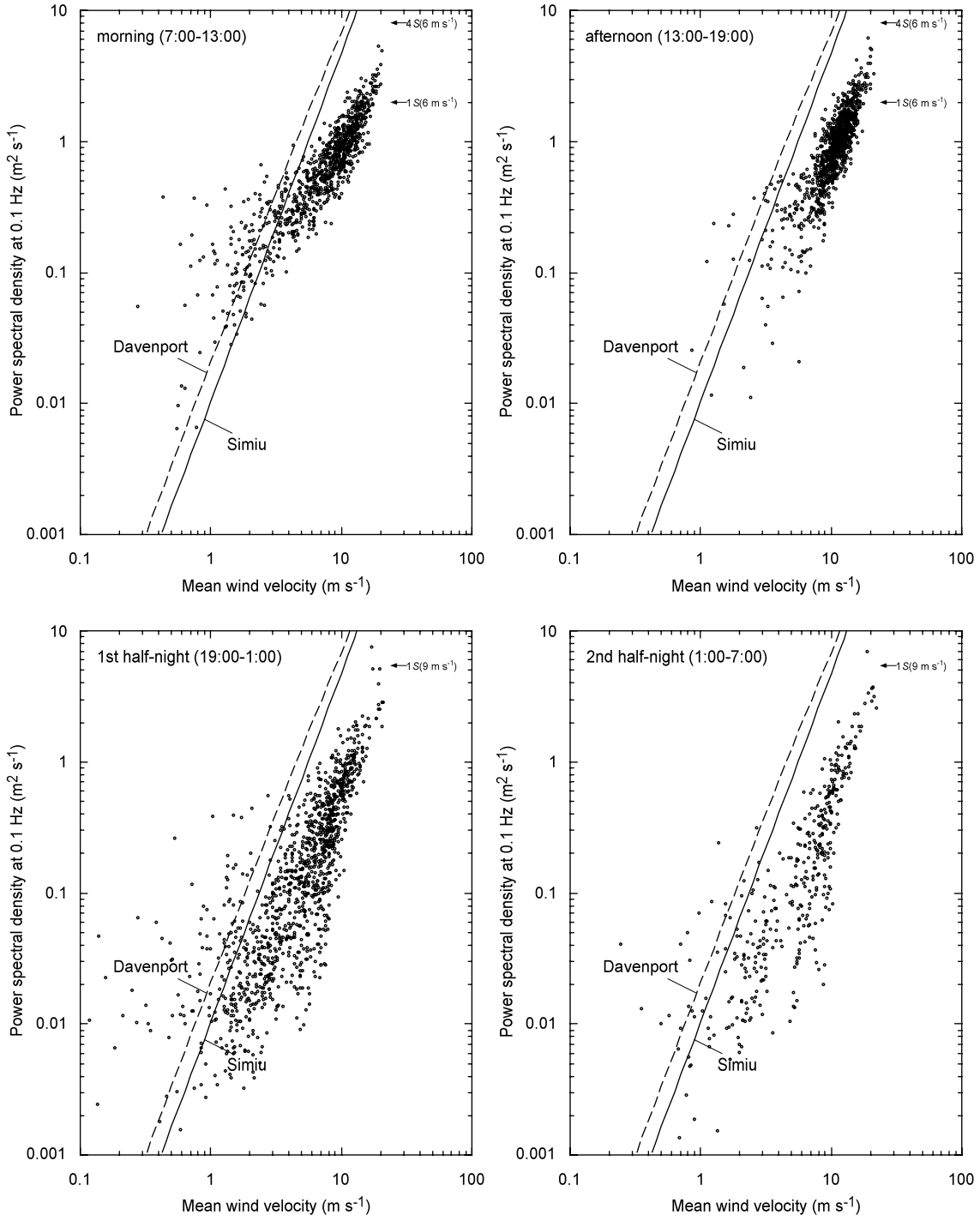

Figure 12: Median wind power spectral density at 0.1 Hz as a function of mean wind velocity for morning (UT − 4h = 7:00–13:00), afternoon (13:00–19:00), first half-night (19:00–1:00), and second half-night (1:00–7:00). Diagonal lines represent the prediction of the Simiu model (*solid line*) and the Davenport model (*dashed line*) under the roughness length of 0.05 m, and horizontal arrows correspond to the levels of the power spectral density in the Simiu spectra under the daytime condition ($\bar{v} = 6\,\mathrm{m\,s^{-1}}$, S and $4S$) and nighttime condition ($\bar{v} = 9\,\mathrm{m\,s^{-1}}$, S) assumed in the antennas' technical specification. The power spectral density for additional assumed nighttime condition ($\bar{v} = 9\,\mathrm{m\,s^{-1}}$, $4S$) falls out of the plot area and no data exceeds this value.

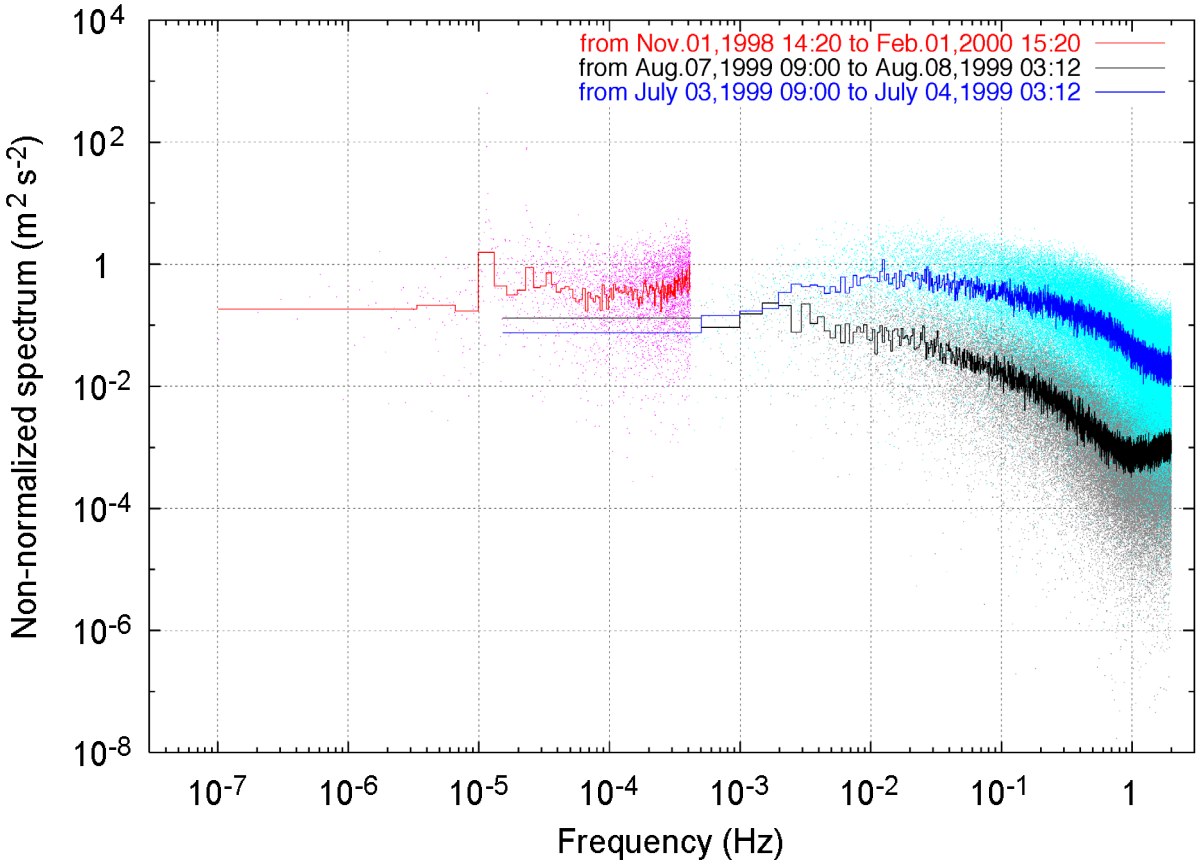

Figure 13: Non-normalized wind spectrum in macro- through micro-meteorological range ("van der Hoven spectrum"). The spectrum up to 0.0004 Hz (40 min) was extracted from the weather station data taken during a period from 1998 November 1 to 2000 February 1 (*red*). Overlaid spectra in higher frequency range were extracted from the N-800S anemometer data during the windy 18.2-hr period starting from 9:00 of 1999 July 3 (*blue*) and the calm period starting from 9:00 of 1999 August 7 (*black*).